Synthesis and *in situ* transformation of PST-1: a potassium gallosilicate natrolite with a high Ga content

Jiho Shin,[a] Seok Han Kim,[a] Miguel A. Camblor,[b] Stewart J. Warrender,[c] Stuart R. Miller,[c] Wuzong Zhou,[c] Paul A. Wright[c] and Suk Bong Hong*[a]

Received (in XXX, XXX) Xth XXXXXXXXX 200X, Accepted Xth XXXXXXXXX 200X
First published on the web Xth XXXXXXXXX 200X
DOI: 10.1039/b000000x

The synthetic details of a novel potassium gallosilicate natrolite with Si/Ga = 1.28, denoted PST-1, are described. The presence of K^+ and Ga with well-defined levels of concentration in the synthesis mixture is essential for directing its crystallization. PST-1 transforms rapidly into TNU-6 under hydrothermal conditions, behavior that contrasts sharply with its very high thermal and hydrothermal stability, which is unusual for a material of such a high Ga content. These stability issues are discussed and rationalized based on chemical composition, likely violations of Loewenstein's rule and the temperature of dehydration of as-made K-PST-1. The crystal structure of TNU-6 has been resolved through the combined use of synchrotron X-ray and electron diffraction data; it has the $BaFeGaO_4$ structure type with an additional $\sqrt{3}a \times \sqrt{3}a$ '$KGeAlO_4$' superstructure that arises from tilting of some of the tetrahedral units in all of the 6-rings.

Introduction

There are still strong driving forces for developing zeolites and other molecular sieves with novel framework structures and/or compositions, because they offer valuable opportunities in developing new processes based on shape selective effects, as well as in improving existing ion exchange, catalysis and separation technologies. Over the past three decades, in fact, both structural and compositional regimes of crystalline, microporous materials have been greatly extended,[1] largely due to the development of more efficient and innovative synthetic strategies based on understanding the role of inorganic/organic structure-directing agents (SDAs) and the process by which they affect the formation of the final crystalline structure.

The natural zeolite natrolite (framework type NAT) is a three-dimensional, small-pore material with intersecting 8-ring (2.6 x 3.9 Å) and 9-ring (2.5 x 4.1 Å) channels, and a number of compositions of this family of zeolites incorporating Al, Ga and Ge in the tetrahedral sites (T-sites) have been reported.[1,2] PST-1 (**POST**ECH number 1) is a new potassium gallosilicate natrolite with the typical chemical composition $K_{17.54}Ga_{17.54}Si_{22.46}O_{80}{\cdot}16.4H_2O$ with (*Fdd*2) symmetry that we have very recently crystallized.[3] It is characterized by its unusually low Si/Ga ratio (1.28), which is considerably lower than the T^{4+}/T^{3+} ratios ($\geq$ 1.5) of all known NAT materials, with the exception of the natural mineral gonnardite with Si/Al ~ 1.2 and a high concentration of Ca^{2+} ions.[4] Nevertheless, PST-1 is thermally stable up to at least 800 °C. Also, it can withstand hydrothermal treatments up to at least 600 °C in the presence of 10% water vapor. These results are in sharp contrast with the behavior of its more siliceous sodium gallosilicate counterparts with Si/Ga ~ 1.6 that lose crystallinity upon exposure to ambient air after heating at temperatures below 400 °C.[5-7]

The most striking feature of PST-1 is its ability to selectively adsorb the smallest gases, He and especially H_2, with Lennard-Jones (L-J) diameters of 2.60 and 2.89 Å, respectively. PST-1 can discriminate them from slightly larger molecules such as Ar and CO_2 with L-J diameters of 3.40 and 3.30 Å, respectively, making this Ga-rich material a potential candidate for fast, selective H_2 or He separation processes based on pressure swing adsorption or membrane technology.[3] Here we describe our detailed study on the hydrothermal synthesis of PST-1 in the presence of K^+ ions as an inorganic SDA, revealing that it is kinetically driven. With prolonged heating in the K^+-containing crystallization medium, PST-1 was found to transform rapidly into TNU-6 (**T**aejon **N**ational **U**niversity number 6), one of a series of gallosilicate materials that we have previously prepared without the use of any organic additive.[6] The crystal structure of TNU-6 has been solved by combining synchrotron powder diffraction and transmission electron microscopy, and its physical properties have been characterized by using elemental and thermal analyses, high-temperature powder X-ray diffraction, scanning electron microscopy, and ^{29}Si and ^{71}Ga MAS NMR.

Experimental

Synthesis

[a] *School of Environmental Science and Engineering and Department of Chemical Engineering, POSTECH, Pohang 790-784, Korea. E-mail: sbhong@postech.ac.kr*
[b] *Instituto de Ciencia de Materiales de Madrid, Consejo Superior de Investigaciones Científicas (CSIC), C/Sor Juana Inés de la Cruz, 3, 28049 Madrid, Spain, and School of Chemistry*
[c] *School of Chemistry, University of St. Andrews, Purdie Building, North Haugh, St. Andrews KY16 9ST, UK*

†Electronic Supplementary Information (ESI) available: Powder XRD and SEM image, TGA/DTA curves, synchrotron powder diffraction data, ^{71}Ga MAS NMR spectrum, See DOI: 10.1039/b000000x

In a typical synthesis of gallosilicate materials, gallium oxide (Ga_2O_3, 99.99+%, Aldrich) was first mixed with a solution of KOH (45% aqueous solution, Aldrich) in water. Then, the mixture was heated overnight at 100 ºC. After cooling to room temperature, a given amount of colloidal silica (Ludox AS-40, DuPont) was added to this translucent solution. The gel composition of the resulting mixture was $x K_2O{\cdot}y Ga_2O_3{\cdot}10.0SiO_2{\cdot}150H_2O$, where x and y are varied between $8.0 \leq x \leq 12.0$ and $0 \leq y \leq 4.0$, respectively. For comparison, experiments where KOH was replaced by equivalent amount of NaOH (50% aqueous solution, Aldrich), RbOH (50% aqueous solution, Aldrich), or CsOH (50% aqueous solution, Aldrich) were also carried out. The final synthesis mixture was stirred at room temperature for 1 day, charged into Teflon-lined 23-mL autoclaves, and heated at 150 ºC under rotation (60 rpm) for 1-35 days. The solid products were recovered by filtration, washed repeatedly with water, and then dried overnight at room temperature. For the synthesis of aluminosilicate materials, aluminum hydroxide ($Al(OH)_3{\cdot}1.0H_2O$, Aldrich) instead of Ga_2O_3 was dissolved in an aqueous KOH solution. The subsequent steps were the same as those in the procedures given above. If required, PST-1 seed crystals (10 wt% of the silica in the gel) were added to the aluminosilicate synthesis mixture. For comparison, the orthorhombic (*Fdd*2) member (Si/Ga = 1.57, with a high degree of ordering) of the NAT family of sodium gallosilicate zeolites was prepared at 200 ºC under rotation (60 rpm) for 14 days.[6] Here we refer to this material as our previous laboratory code TNU-4 for the sake of clarity and distinction from PST-1. As-made PST-1 and TNU-4 in the K^+ and Na^+ forms were refluxed four times in 1.0 M $NaNO_3$ and 1.0 M KNO_3 solutions (2.0 g solid per 100 mL solution) for 6 h, respectively, in order to maximize the concentration of the exchanging cations in these two materials.

Analytical methods

Phase identity and purity of the solid products were checked by powder X-ray diffraction (XRD) on a PANalytical X´Pert diffractometer with an X´Celerator detector. Data were collected with a fixed divergence slit (0.50º) and Soller slits (incident and diffracted = 0.04º) and Cu K_α radiation. *In situ* high-temperature XRD experiments were performed in Bragg-Brentano geometry using the same diffractometer equipped with an Edmund Bühler HDK 1.4 high-temperature attachment. Elemental analysis was performed by a Jarrell-Ash Polyscan 61E inductively coupled plasma (ICP) spectrometer in combination with a Perkin-Elmer 5000 atomic absorption spectrophotometer. Thermogravimetric and differential thermal analyses (TGA/DTA) were performed in air on an SII EXSTAR 6000 thermal analyzer. Crystal morphology and size were determined by a JEOL JSM-6300 scanning electron microscope (SEM). The ^{29}Si MAS NMR spectra were measured on a Bruker DSX 400 spectrometer at a spinning rate of 12.0 kHz using 4 mm rotors at a ^{29}Si frequency of 79.490 MHz with a $\pi/5$ rad pulse length of 2.0 μs. The recycle delay for ^{29}Si NMR spectra was varied between 40 and 60 s to avoid relaxation effects in the signal intensities. Typically, 1000 pulse transients were accumulated and the ^{29}Si chemical shifts are referenced to TMS. Spectral deconvolution and simulation were performed using the PeakFit curve-fitting software. The ^{71}Ga MAS NMR spectra were obtained on the same spectrometer at a ^{71}Ga frequency of 122.040 MHz in 4 mm rotors at a spinning rate of 10.0 kHz. The spectra were obtained with an acquisition of *ca*. 15,000 pulse transients, which was repeated with a $\pi/4$ rad pulse length of 1.0 μs and a recycle delay of 0.1 s. The ^{71}Ga chemical shifts are reported relative to a $Ga(H_2O)_6^{3+}$ solution.

The high-resolution powder XRD pattern for as-made TNU-6 was collected at –173 ˚C on station ID-31 at ESRF (Grenoble, France) using monochromated radiation with a wavelength of 0.8002 Å. The sample was first loaded in a 0.5 mm quartz glass capillary and dehydrated at 200 ˚C on a glass line at 10^{-4} Torr before sealing. Fourteen data collection were carried out on freshly exposed portions of the sample in Debye–Scherrer geometry, each over 140 s with 2θ of 4–45º, and all data sets were summed. The extraction of the peak positions for indexing was performed using the WinPLOTR program.[8] Pattern indexing was carried out with the computer program DICVOL04 from the first 20 lines, with an absolute error on peak positions of 0.01º 2θ. A hexagonal solution was found with satisfactory figures of merit and confirmed by successful indexing of all input 55 lines in the supercell (18.171 Å × 18.171 Å × 8.511 Å), including the supercell reflections. Systematic absences were consistent with several space groups ($P6_3$, $P6_3/m$, $P6_322$). Subsequent structure solution calculations were performed with the EXPO2004 package[9] in the space group $P6_3$. A list of 586 reflections was extracted in the angular range 4–40º 2θ. According to the degree of diffraction overlap, 44.7% of these reflections were statistically considered as independent. The corresponding atomic co-ordinates were used as the starting model for Rietveld refinement,[10] using the GSAS program suite,[11] over the full extent of the diffraction profile. A pseudo-Voigt function[12] was selected to describe individual line profiles. Unit cell and instrumental parameters were allowed to vary during the refinement process, as well as atomic coordinates (the latter without any distance or angular constraints). A single refined displacement parameter was used for all atoms. The occupancy of tetrahedral Si and Ga sites was fixed according to the chemical composition (the Si sites fully occupied, Ga sites occupied by 97% Ga and 3% Si) and the occupancy of K^+ sites was refined (capped at 1 where appropriate) giving a composition of $K_{0.97}Ga_{0.97}Si_{1.03}O_4$. Use of the PLATON program[13] on the final refined coordinates indicated that there was no additional symmetry above $P6_3$. The final fit to the data was satisfactory (R_{wp} = 7.4%, R_p = 5.7%). Evidence for the presence of a supercell in TNU-6 was also obtained from the electron diffraction (ED) data recorded on a JEOL 2011 transmission electron microscope (TEM) operating at an accelerating voltage of 200 kV.

Results and discussion

Table 1 lists the representative products obtained from synthesis mixtures with the oxide composition $8.0K_2O{\cdot}xMe_2O_3{\cdot}10.0SiO_2{\cdot}150H_2O$ in which x is varied between $0 \leq x \leq 4.0$ and Me is Ga or Al. In each case, the phases listed were the only ones obtained in repeated trials. Crystallization of pure PST-1 was possible only from synthesis mixtures with SiO_2/Ga_2O_3 = 5-10 when carried out at 150 ºC for 2 days. Table 1 also shows that the two PST-1

Table 1 Syntheses from oxide composition $8.0K_2O{\cdot}xMe_2O_3{\cdot}10.0SiO_2{\cdot}150H_2O$[a]

SiO_2/Me_2O_3 ratio in the gel	product[b,c]			
	Me = Ga		Me = Al	
	t = 2 days	t = 14 days	t = 2 days	t = 14 days
2.5	PST-1+U	PST-1+U+(TNU-6)	merlinoite	merlinoite
5	PST-1(1.28)	TNU-6(1.05)	merlinoite	merlinoite
5			merlinoite[d]	
10	PST-1(1.28)	TNU-6(1.06)	merlinoite	merlinoite
20	-[e]	-[e]	merlinoite	merlinoite
∞		-[e]		

[a] x is varied between $0 \le x \le 4.0$ and Me is Ga or Al. Crystallization was performed under rotation (60 rpm) at 150 ºC. [b] The phase appearing first is the major phase, and the product obtained in a trace amount (< 5 %, according to powder XRD analysis) is given in parentheses. U is an unknown but probably dense material. [c] The values in parentheses are bulk Si/Ga ratios of the product, as determined by elemental analyses. [d] The material prepared by adding a large amount (10 wt% of the silica in the gel) of gallosilicate PST-1 as seeds to the aluminosilicate synthesis mixture. [e] No solids were obtained.

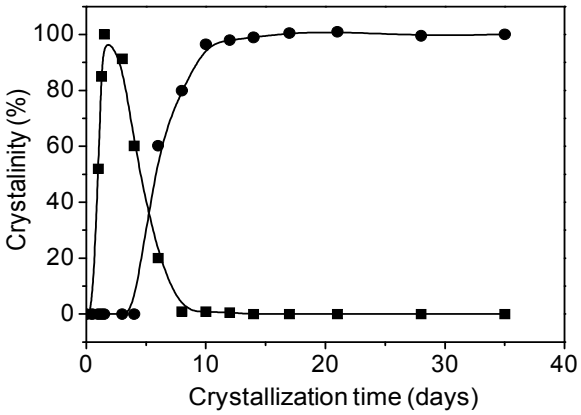

Fig. 1 Crystallinity of PST-1 and (■) TNU-6 (●) as a function of crystallization time from a synthesis mixture with the chemical composition $8.0K_2O{\cdot}1.0Ga_2O_3{\cdot}10.0SiO_2{\cdot}150H_2O$ at 150 ºC under rotation (60 rpm).

samples prepared at SiO_2/Ga_2O_3 ratios of 5 and 10, respectively, have the same bulk Si/Ga ratio (1.28). Thus, a specific level of Ga concentration in the synthesis mixture appears to be essential for crystallizing PST-1 in the presence of K^+ ions as a SDA. As previously reported,[6] however, an increase of crystallization time to 14 days at the same temperature led to the formation of TNU-6 as a minor or sole phase whose crystal structure has remained unresolved thus far. It is interesting to note here that synthetic sodium gallosilicate natrolites with Si/Ga ratios close to but slightly larger than 1.50 maintain their structural integrity at 150 ºC or higher for 4 weeks in the crystallization medium, although there is a slow change in the distribution of Si and Ga of the NAT framework from a disordered phase to a ordered one, together with a change from tetragonal to orthorhombic symmetry.[7]

In our view the low thermodynamic stability of PST-1 in the crystallization medium may be due to its Si/Ga ratio being much smaller than 1.5, which may cause a significant concentration of violations of the extended Loewenstein's rule, *i.e.* the avoidance of T^{3+}-O-T^{3+} pairings in tectosilicates. In fact, PST-1 presents some degree of order in the occupancy of T-sites by Si and Ga[3] that may not be compatible with a full observance of the rule in a NAT topology with Si/Ga < 1.5.[14] This ordering causes PST-1 to adopt an *Fdd*2 orthorhombic symmetry rather than the tetrahedral $I\bar{4}2d$ symmetry characteristic of natrolites with a disordered distribution of Si and Ga over T-sites.[7] The existence of Ga-O-Ga pairs could help explain the small but significant disagreement between the Si/Ga ratios obtained by chemical analysis (1.28) and ^{29}Si MAS NMR spectroscopy (1.39), as recently reported.[3] Given that materials that do not obey the Loewenstein's rule actually exist,[15-17] the rule may constitute usual behavior, but cannot be regarded as an unavoidable constraint. In fact, according to recent Monte Carlo simulations,[7] disordered gallosilicate natrolites with Si/Ga slightly over 1.5 exhibit violations of the Loewenstein's rule, which convey an energy penalty that is likely to be responsible for their transformation into their ordered counterparts under crystallization conditions. Unfortunately, evidence for Ga-O-Ga pairs is most difficult to obtain and may require triple-quantum ^{17}O MAS NMR experiments after very expensive ^{17}O enrichment of PST-1. Nonetheless, it appears sensible to us that Ga-O-Ga pairs exist in PST-1 and that the energetic cost associated with these "defects" may drive its transformation to TNU-6 under synthesis conditions.

Fig. 1 shows the crystallization curve of PST-1 from the oxide composition $8.0K_2O{\cdot}1.0Ga_2O_3{\cdot}10.0SiO_2{\cdot}150H_2O$ at 150 ºC under rotation (60 rpm). PST-1 is the phase that crystallizes first. Then, TNU-6 begins to grow rapidly at the expense of PST-1 and is fully crystallized after about 10 days of heating. This gallosilicate solid was found to be stable for at least additional 3 weeks of heating in the crystallization medium. Therefore, it is most likely that PST-1 has a much lower activation energy for nucleation than TNU-6, making its formation kinetically favored. As seen in Table 1, on the other hand, a decrease of the SiO_2/Ga_2O_3 ratio in the synthesis mixture from 10 to 2.5 slowed down the crystallization of PST-1. When the initial SiO_2/Ga_2O_3 ratio in the synthesis mixture is higher than 10, by contrast, no solid products were obtained even after 14 days of heating in the crystallization medium. When changing the trivalent, tetrahedral lattice-substituting component from Ga to Al, in particular, we always obtained merlinoite (MER) at SiO_2/Al_2O_3 ratios ≤ 20. The same result was observed even when a large amount (10 wt% of the silica in the gel) of gallosilicate PST-1 is added as seeds to the aluminosilicate synthesis mixture. This again shows that crystallization of PST-1 is highly sensitive both to the presence of Ga and its concentration. We should note here that decreasing and increasing K_2O/SiO_2 ratio in the gel with SiO_2/Ga_2O_3 = 10 from 0.8 to ≤ 0.6 and 1.0 result in the crystallization of TNU-1 (CGS)[14] and TNU-6 after 2 days of heating, respectively. We also found that the replacement of KOH with the equivalent amount of NaOH under the conditions (SiO_2/Ga_2O_3 = 5 and K_2O/SiO_2 = 0.8) where the crystallization of PST-1 under rotation (60 rpm) proved to be reproducible yielded gallosilicate sodalite (SOD), while the use of both RbOH and CsOH gave gallosilicate analcime (ANA). Therefore, it is clear that the type and concentration of alkali cations in the synthesis mixture is another critical factor governing the synthesis of PST-1. A similar trend has also been

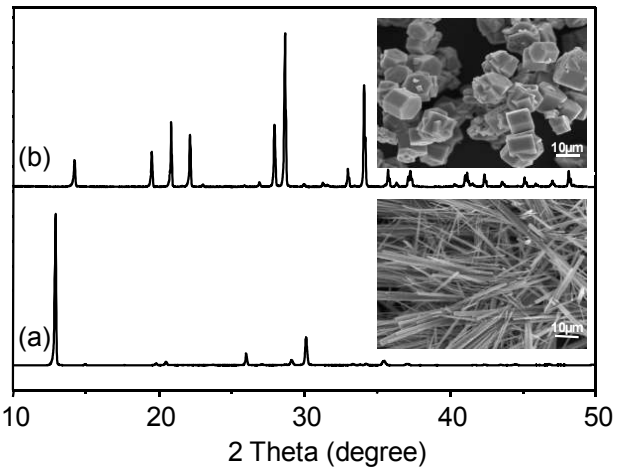

Fig. 2 Powder XRD patterns and SEM images of PST-1 and TNU-6 obtained after heating a synthesis mixture with SiO_2/Ga_2O_3 = 10 and K_2O/SiO_2 = 0.8 under rotation (60 rpm) at 150 ºC for (a) 2 and (b) 14 days.

observed in the synthesis of other structure types of gallosilicate zeolites such as TNU-1, TNU-7 (EON), and ECR-34 (ETR).[5,18-22]

Fig. 2 shows the powder XRD patterns and SEM images of PST-1 and TNU-6 obtained by heating a synthesis mixture with SiO_2/Ga_2O_3 = 10 and K_2O/SiO_2 = 0.8 at 150 ºC for 2 and 14 days, respectively (Table 1). Although the pattern of PST-1 shows preferred orientation that can be attributed to the needle-like crystal morphology observed by SEM (Fig. 2), we note that it is very similar to that of the K^+ ion-exchanged form (*i.e.*, K-TNU-4) of the almost ordered orthorhombic gallosilicate with the NAT topology prepared in the presence of Na^+ ions.[6] This is due to the similar unit cell parameters and symmetry of both orthorhombic potassium natrolites. It is also remarkable that the PST-1 crystals obtained at a lower SiO_2/Ga_2O_3 ratio (5) are characterized by a considerably smaller aspect ratio (*ca*. 8 vs *ca*. 24), while there are no differences in the Si/Ga ratio (ESI† Fig. S1). This suggests that the crystal growth rate along [001] decreases relative to the rate along [100] and [010] as the Ga concentration in solution increases.

Our recent analysis of the synchrotron X-ray powder diffraction data reveals that the refined unit cell parameters of as-made PST-1 are *a* = 19.3148(2) Å, *b* = 19.2482(2) Å, *c* = 6.53313(5) Å (*Fdd*2).[3] A combination of elemental and thermal analyses indicates, within experimental error, that this small-pore material has the unit cell composition $K_{17.54}Ga_{17.54}Si_{22.46}O_{80}\cdot 16.4H_2O$. We should note here that PST-1 contains two-thirds of the amount of water molecules of the aluminosilicate gonnardite ($Na_{6.42}K_{0.01}Ca_{1.50}Al_{9.22}Si_{10.73}O_{40}\cdot 12.37\ H_2O$),[4] probably due to the larger size and concentration of countercations (K^+) in the former compared to those (mainly Na^+ and Ca^{2+}) in the latter. However, we found that despite the notable difference (1.28 vs 1.57) in their Si/Ga ratios,[7] PST-1 and K-TNU-4 are characterized by similar unit cell volumes (2428.9 and 2468.2 $Å^3$). There is only a 1.6% volume difference for a 12.7% difference in Ga content. When compared to the latter material with the chemical composition $K_{15.40}Na_{0.16}Ga_{15.56}Si_{24.44}\ O_{80}\cdot 17.6H_2O$ and unit cell parameters *a* = 19.090 Å, *b* = 19.824 Å, *c* = 6.522 Å, however, a

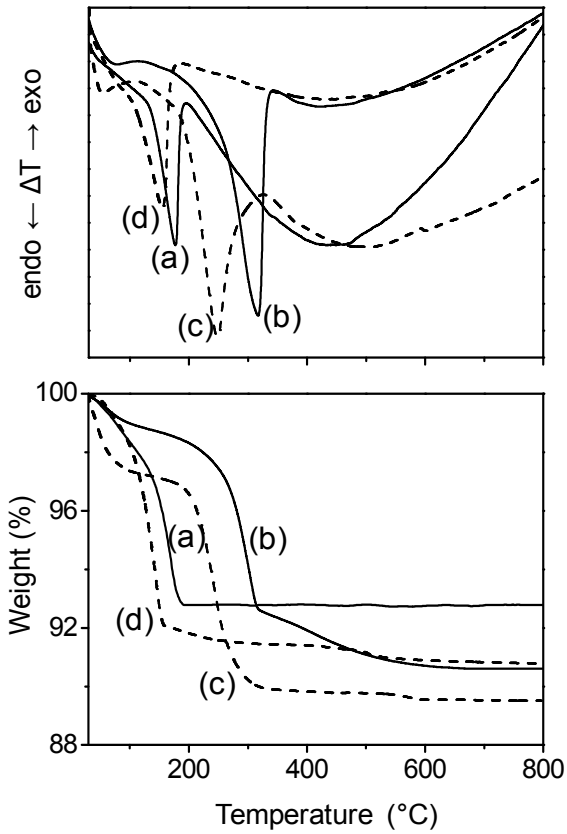

Fig. 3 TGA (bottom) and DTA (top) curves for (a) as-made K-PST-1 and (b) as-made Na-TNU-4, (c) Na^+-exchanged PST-1, and (d) K^+-exchanged TNU-4.

lower water content, as well as a higher Ga content, is observed for the former material, which appears to result in a unit cell with slightly longer *a* and *c* and much shorter *b* dimensions. It is very frequent in zeolite science that claims of isomorphous substitutions are allegedly supported by changes in the unit cell dimensions, so that an increase in volume for a material with a larger concentration of larger heteroatoms is taken as an evidence of the substitution. The case shown here for PST-1 and K-TNU-4 makes clear how flawed this approach may be. In fact, silica-rich ($5.7 \leq Si/Al \leq 23$) aluminosilicate sodalite materials have shown to be an extreme case in which a change in the orientation of framework tetrahedra results in volume changes opposite to the expected trend.[23,24]

Fig. 3 compares the TGA/DTA curves for as-made K-PST-1, Na-TNU-4, and their Na^+- and K^+-exchanged forms. While the weight loss (7.8 vs 7.2 wt%) due to the desorption of occluded water is slightly larger for TNU-4 than for PST-1, the temperature (360 vs 175 ºC) of the endothermic peak maxima in the DTA is markedly lower (by 185 ºC) for the latter material. Therefore, it is clear that the material with a higher Ga content dehydrates more easily than TNU-4 with a lower content. This can be rationalized by suggesting that the interaction of water molecules with larger K^+ ions may be much weaker than that with Na^+ ions, because the Na-PST-1 sample with a Na^+ ion exchange level of 95%, according to ICP analysis, gives an endotherm around 250 ºC, *i.e.*, 75 ºC above its parent material. Additionally, the TGA curves in Fig. 3 indicate that the amount (23.0

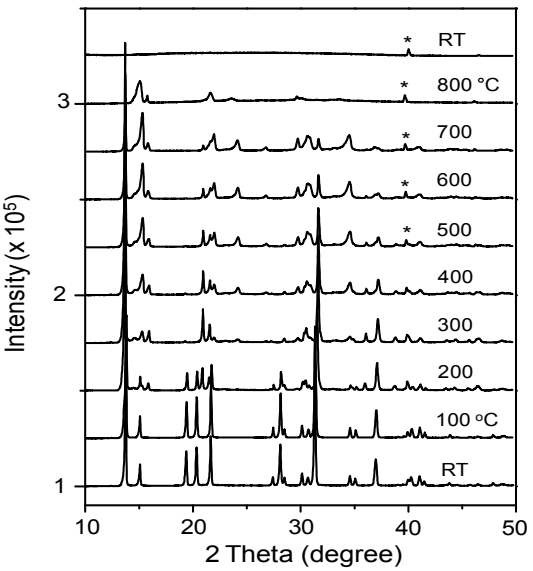

Fig. 4 Powder XRD patterns of Na-PST-1 measured during *in situ* heating under vacuum to a residual pressure of 5×10^{-3} Torr. The top trace is the pattern measured at room temperature after temperature-programmed XRD experiments up to 800 ºC followed by exposure to ambient air for 0.5 h. The asterisk denotes an X-ray peak from the Pt sample holder.

H_2O/40T) of water retained in the Na^+-exchanged form is considerably larger than that (16.4 H_2O/40T) in the as-made K^+ form. The *in situ* high-temperature XRD patterns of Na-PST-1 recorded under vacuum (5×10^{-3} Torr) are shown in Fig. 4. Unlike its parent material (*i.e.*, K-PST-1) that withstands thermal and 10% steam treatments up to at least 800 and 600 ºC, respectively,[3] Na-PST-1 is already much modified at 300 ºC. When exposed to ambient for 0.5 h after temperature-programmed XRD experiments up to 800 ºC, in particular, it completely loses crystallinity. Furthermore, the (hydro)thermal behavior of as-made K-PST-1 with a large Ga content (Si/Ga = 1.28) sharply contrast with that of its more siliceous sodium gallosilicate NAT counterparts with smaller Ga contents (Si/Ga ~ 1.6), which require dehydration temperatures of 350 ºC or higher and become amorphous upon exposure to ambient air.[7] To date, there are two other gallosilicate natrolites prepared in the presence of K^+ ions as a SDA:[25,26] the tetragonal ($I42d$) $K_8Ga_8Si_{12}O_{40}{\cdot}6H_2O$ and orthorhombic ($I2_12_12_1$) $K_{8.2}Ga_{8.2}Si_{11.8}O_{40}{\cdot}11.5H_2O$ phases. Since the latter phase was claimed to have a Si/Ga ratio of 1.44 only from relatively inaccurate selected area energy dispersive X-ray analysis,[26] however, it is still unclear whether its Si/Ga ratio is really below 1.5, like the case of PST-1. Besides differences in the crystal symmetry and unit cell composition, furthermore, this orthorhombic phase shows significant differences in the rehydration behavior compared to that of PST-1. While its dehydrated form can turn back to the original state when exposed to ambient for a week or longer,[26] the dehydrated PST-1 sample is almost fully rehydrated within 1 h upon exposure to the laboratory humidity conditions.

The fact that PST-1 with a lower Si/Ga ratio (~ 1.3) is (hydro)thermally more stable than other synthetic gallosilicate natrolites with higher Si/Ga ratios (≥ 1.5) reported thus far[5,7] is in contrast with the general expectation, because the thermal stability of zeolites normally improves upon increasing their Si/T^{3+} ratio.[27] In the following, we advance a hypothetical explanation for this unexpected observation based on the observed ease of dehydration of PST-1. If the breaking and reorganization of Ga-O-Si bonds is hydrolytic, *i.e.*, if it involves the water-mediated breaking of Ga-O-Si bonds with formation of Ga-OH and Si-OH groups, it would then require the presence of some water, together with some thermal energy. Since essentially all water in PST-1 is lost at a very low temperature (*e.g.*, 60 ºC in vacuum and < 200 ºC in air) when the system reaches a temperature high enough to break bonds, the material is completely dehydrated, making its reorganization no longer possible or extremely slow. By contrast, the materials (*e.g.*, Na-TNU-4) which still have some water at temperatures ≥ 300 ºC,[7] high enough to break bonds, can undergo a reorganization and hence show a lower thermal stability, despite their higher Si/Ga ratio. Once the formation of Ga-OH and Si-OH groups has started, this "bonded water", which is not so easily removed, may allow the reorganization of Ga-O-Si bonds to propagate: after dehydration of a Ga-OH/Si-OH couple, the water produced may break another Ga-O-Si bond and so on. In support of this hypothesis, we have checked that K^+-exchanged TNU-4, which also dehydrates easily, shows an improved thermal stability compared to its as-made Na^+ form. As seen in Fig. 4, however, Na^+-exchanged PST-1, which dehydrates at a higher temperature, is thermally less stable than as-made K-PST-1.

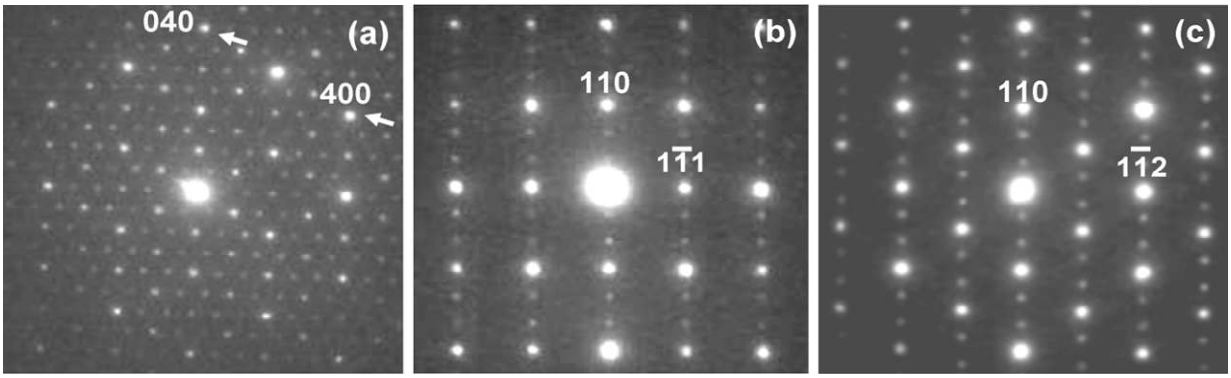

Fig. 5 Selected area diffraction patterns of TNU-6 taken down the (a) [001], (b) [$\bar{1}$12] and (c) [$\bar{1}$11] zone axes. The patterns are indexed on the 10.525 Å x 10.525 Å x 8.538 Å subcell. The presence of the √3a supercell reflections is clearly visible.

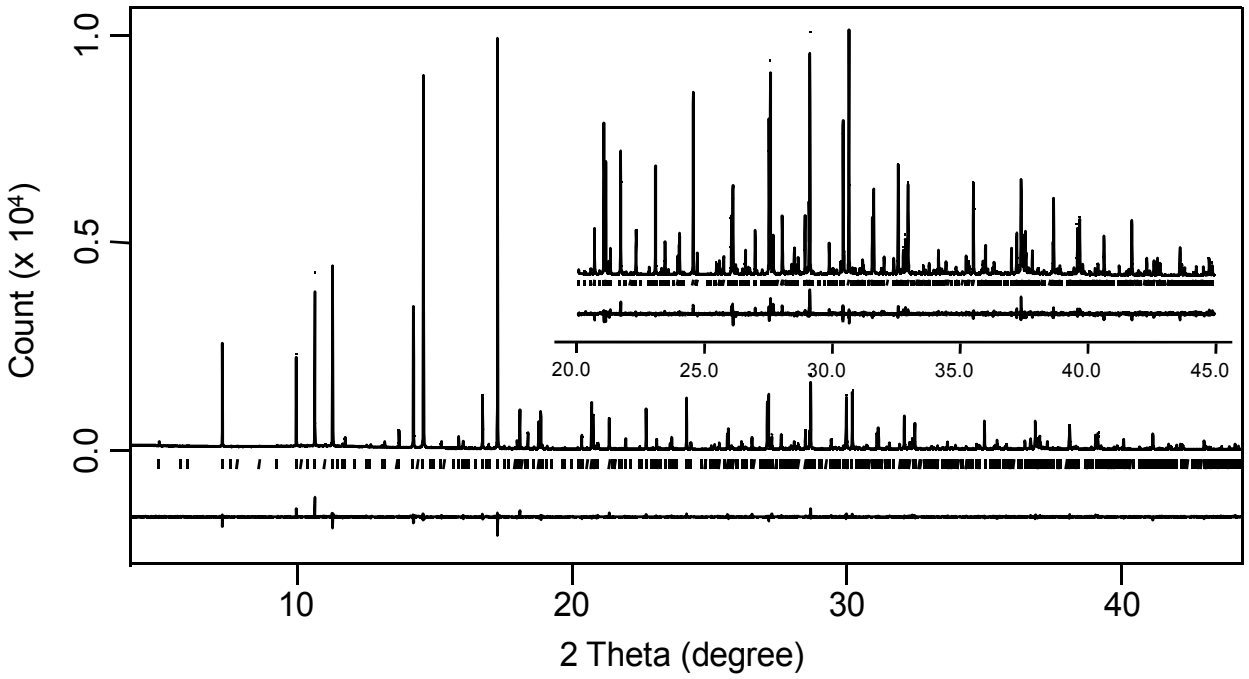

Fig. 6 Rietveld plot for TNU-6: observed data (crosses), calculated profile (solid line), and difference (lower line). Vertical ticks indicate the positions of allowed reflections.

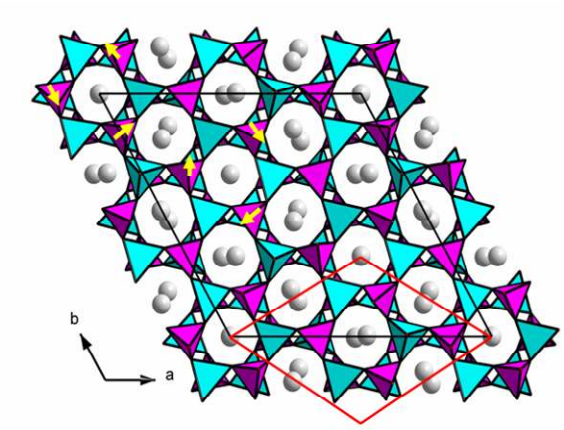

Fig. 7 Refined structure of TNU-6 viewed along the c-axis with $BaFeGaO_4$-type cell overlain in red. SiO_4 tetrahedra are represented in purple, and (predominantly) GaO_4^- tetrahedra in cyan. The variation in tilting of tetrahedral units is indicated by yellow arrows.

Fig. 2 above shows that the positions and relative intensities of all the X-ray peaks from TNU-6 are essentially the same as those reported in our preliminary study.[6] The observed hexagonal prismatic crystal morphology is also consistent with the symmetry determined crystallographically (see below). No noticeable weight loss at temperatures up to 800 ºC was observed from its TGA/DTA curves (ESI† Fig. S2). TNU-6 was determined to have the oxide composition $K_{23.3}Ga_{23.3}Si_{24.7}O_{96}$ (based on the hexagonal unit cell of the as-made material) from elemental analysis. The transformation of PST-1 into TNU-6 is a solution-mediated solution-recrystallization process, given the observed changes in chemical composition and crystal size and morphology between both materials. The more stable TNU-6 has the '$KGeAlO_4$/$BaFeGaO_4$' framework type,[27] which is related to the well-known kalsilite ($KAlSiO_4$) 'stuffed tridymite' structure type, which has a dense, fully tetrahedrally-connected framework but with different orientations of some of the tetrahedral units.

Fig. 5 shows three selected area electron diffraction (SAED) patterns of TNU-6, viewed down the [001], [$\bar{1}$12], and [$\bar{1}$11] zone axes of the hexagonal basic cell with a = 10.5 Å and c = 8.5 Å, respectively, typical of the $BaFeGaO_4$ structure type.[28] However, there are also weaker diffraction maxima, indicating a hexagonal supercell via rotating the a axis of the basic cell by 30º and a supercell with $\sqrt{3}a$ x $\sqrt{3}a$ x c dimensions. Since these weak diffraction peaks were not visible in the laboratory powder XRD data, we carried out synchrotron diffraction measurements on TNU-6 and were able to find the supercell reflections (ESI† Fig. S3). It was also possible to solve the structure from the synchrotron powder diffraction data and to refine it satisfactorily in the larger supercell, despite the large number of atomic coordinate variables. The final atomic positions for TNU-6 are listed in Table 2 with the final Rietveld plot in Fig. 6.

Fig. 7 shows the finally refined structure of TNU-6 with the $KAlGeO_4$-type hexagonal unit cell.[29,30] In this structure the framework has the same arrangement of tetrahedral units as found in $BaFeGaO_4$ (there are two arrangements in the 6-rings, UDUDUD and UUUDDD[31]) but with an additional supercell created by a variation in the direction of tilt of tetrahedral units within the UDUDUD rings. Instead of tilting all in the same sense around the rings, as is the case in $BaFeGaO_4$, in the $KAlGeO_4$ structure (which is adopted here by $KGaSiO_4$) one half of these rings tilt in the opposite sense. K^+ ions are located at occupancies of 1 or close to 1 in six different sites, each of which lies between two 6-rings in different layers. The fact that the occupancies of some of the K^+ sites are less than 1 is required by charge balance considerations for a sample with Si/Ga > 1. The $KAlGeO_4$ structure type has been reported for several different compositions, including α-$KZnPO_4$ and α-$KCoPO_4$.[32,33] Barbier,

Table 2 Final atomic coordinates and thermal parameters for TNU-6

atom	*x*	*y*	*z*	occupancy	U_{iso} (x 100 Å^2)
Si1	0.4983(6)	0.1738(7)	0.5650(17)	1	0.21(2)
Si2	0.6574(7)	0.1643(6)	0.0682(15)	1	0.21(2)
Si3	0.6646(9)	-0.0005(7)	0.4518(6)	1	0.21(2)
Si4	0.1663(8)	0.0063(6)	0.5485(15)	1	0.21(2)
Ga1	0.6563(3)	0.1651(3)	0.4494(7)	0.97	0.21(2)
Ga2	0.4995(2)	0.17488(3)	0.9471(7)	0.97	0.21(2)
Ga3	0.3319(4)	-0.0005(3)	0.5621	0.97	0.21(2)
Ga4	0.8325(3)	-0.0052(2)	0.4389(6)	0.97	0.21(2)
Si5	0.6563(3)	0.1651(3)	0.4494(7)	0.03	0.21(2)
Si6	0.4995(2)	0.17488(3)	0.9471(7)	0.03	0.21(2)
Si7	0.3319(4)	-0.0005(3)	0.5621	0.03	0.21(2)
Si8	0.8325(3)	-0.0052(2)	0.4389(6)	0.03	0.21(2)
O1	0.5559(11)	0.1369(13)	0.5667(23)	1	0.21(2)
O2	0.4042(14)	0.1069(130	0.4996(21)	1	0.21(2)
O3	0.4767(10)	0.1935(11)	0.7438(26)	1	0.21(2)
O4	0.5351(14)	0.2616(11)	0.4739(19)	1	0.21(2)
O5	0.6113(10)	0.2068(11)	-0.0279(21)	1	0.21(2)
O6	0.6168(10)	0.1421(10)	0.2461(25)	1	0.21(2)
O7	0.7516(11)	0.2241(12)	0.0612(24)	1	0.21(2)
O8	0.6374(12)	0.0744(12)	-0.0186(27)	1	0.21(2)
O9	0.6789(11)	0.007999)	0.2680(11)	1	0.21(2)
O10	0.5661(14)	-0.0675(14)	0.5186(28)	1	0.21(2)
O11	0.6924(13)	0.0955(15)	0.5198(27)	1	0.21(2)
O12	0.7308(14)	-0.0284(15)	0.5316(24)	1	0.21(2)
O13	0.2248(15)	-0.0332(15)	0.4899(24)	1	0.21(2)
O14	0.1779(11)	0.0419(10)	0.7257(17)	1	0.21(2)
O15	0.0689(12)	-0.0546(13)	0.5189(17)	1	0.21(2)
O16	0.1963(10)	0.0959(9)	0.4496(21)	1	0.21(2)
K1	0.6667	0.3333	0.2416(23)	0.97(1)	0.21(2)
K2	0.3321(7)	0.1452(5)	0.2520(12)	0.930(5)	0.21(2)
K3	0.0	0.0	0.2571(11)	1	0.21(2)
K4	0.1339(4)	0.3289(60	0.2510(12)	0.958(6)	0.21(2)
K5	0.0047(4)	0.4803(6)	0.2544(8)	1	0.21(2)
K6	0.3333	0.6667	0.2431	0.975(12)	0.21(2)

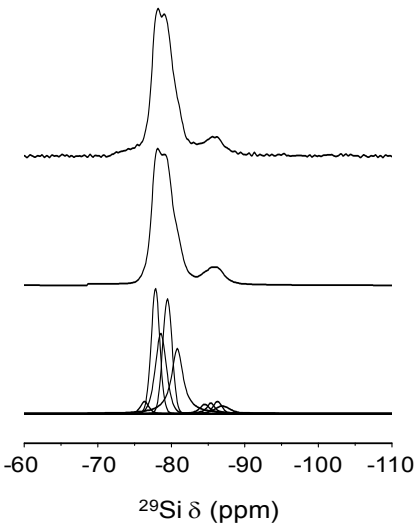

Fig. 8 ^{29}Si MAS NMR spectra of as-made TNU-6: experimental (top); simulated (middle); deconvoluted components (bottom).

and Fleet have speculated that this is also the case of $KGaSiO_4$ without reference to the details of the structure.[34] In their work, the $KGaSiO_4$ was not prepared hydrothermally, but rather from heating pelletized reactants at 900 ˚C and then 1000 ˚C. Therefore, we speculate that the structure-direction to the$KAlGeO_4$ structure type rather than the kalsilite or $BaFeGaO_4$ structure may arise from a subtle interplay between the geometric requirements of T-atoms and interstitial cations. *In situ* high-temperature powder XRD experiments show that TNU-6 is thermally stable under vacuum to a residual pressure of 5×10^{-3} Torr at temperatures at least up to 1000 ºC, which should originate from its nonporous nature.

The ^{71}Ga MAS NMR spectrum (ESI† Fig. S4) of TNU-6 exhibits only one broad asymmetric line around 177 ppm, typical of framework tetrahedral Ga species.[5-7,18-21] The ^{29}Si MAS NMR spectrum of this dense gallosilicate phase, together with the simulated spectrum and its deconvoluted components, is shown in Fig. 8. Four ^{29}Si lines in the region -77 - -81 ppm, which correspond to Si(4Ga) species and must arise from the four sites of equal multiplicity expected from

the TNU-6 crystal structure by a 1:1:1:1 overlap, are distinguishable. As seen in Fig. 8, however, we were able to obtain the best-simulated spectrum by deconvoluting the experimental one into 9 components. Assuming that the lowest-field line around –76 ppm comes from a small amount of amorphous material, a $(Si/Ga)_{nmr}$ ratio of 1.03 was derived from the curve deconvolution. Given that this value matches well with that (1.06) from elemental analysis, ^{29}Si MAS NMR spectroscopy is consistent with the crystal structure of TNU-6 described above.

Conclusion

The synthesis of PST-1, a NAT-type gallosilicate zeolite whose trivalent lattice-substituting heteroatom content (Si/Ga = 1.28) is considerably larger than that of any of the synthetic versions of the same family of zeolites reported thus far, has been reported. It was found that a tetrahedrally-connected potassium gallosilicate framework solid (TNU-6) with the topology of the $BaFeGaO_4$ structure type and the $KAlGeO_4$-type hexagonal supercell readily crystallizes at the expense of PST-1, with prolonged heating in the synthesis medium. The lack of stability of PST-1 under crystallization conditions contrasts with its very high (hydro)thermal stability. In our view, PST-1 contains a non-negligible degree of Ga-O-Ga pairing, violating Loewenstein's rule, with an associated energetic cost that destabilizes this material under synthesis conditions. On the other hand, the ease with which as-made K-PST-1 loses water and the strong framework deformation that closes its pores hinders any hydrolytic transformation upon dehydration. The detailed crystal structure of TNU-6 has been resolved using the powder X-ray and electron diffraction data, and the existence of an additional $\sqrt{3}a \times \sqrt{3}a$ superstructure in TNU-6, which is generated by tilting of some of the tetrahedral units in all 6-rings, has been confirmed. TNU-6 does not contain water in its as-made form and is thermally stable at least up to 1000 °C.

Acknowledgements

This work was supported by KOSEF through the National Research Laboratory Program (R0A-2007-000-20050-0). We thank Prof. A. N. Fitch (ESRF) for help in collecting the synchrotron powder diffraction data.

Notes and references

1 International Zeolite Association, Structure Commission, http://www.iza-structure.org.
2 R. Fricke, H. Kosslick, G. Lischke, M. Richter, *Chem. Rev.*, 2000, **100**, 2303
3 J. Shin, M. A. Camblor, H. C. Woo, S. R. Miller, P. A. Wright and S. B. Hong, *Angew. Chem. Int. Ed*., 2009, **48**, 6647.
4 F. Mazzi, A. O. Larsen, G. Gottardi and E. Galli, *N. Jb. Mineral. Mh*., 1986, 219.
5 H. H. Cho, S. H. Kim, Y. G. Kim, Y. C. Kim, H. Koller, M. A. Camblor and S. B. Hong, *Chem. Mater*., 2000, **12**, 2292.
6 W. C. Paik, M. A. Camblor and S. B. Hong, *Stud. Surf. Sci*., *Catal*. 2001, **135**, [CD-ROM] Paper 05-P-07.
7 S. B. Hong, S.-H. Lee, C.-H. Shin, A. J. Woo, L. J. Alvarez, C. M. Zicovich-Wilson and M. A. Camblor, *J. Am. Chem. Soc*., 2004, **126**, 13742.
8 T. Roisnel and J. Rodriguez-Carvajal, *Mater. Sci. Forum,* 2001, **378-381**, 118.
9 A. Altomare, R. Caliandro, M. Camalli, C. Cuocci, C. Giacovovazzo, A. Grazia, A. G. G. Moliterni and R. Rizzi, *J. Appl. Crystallogr*., 2004, **37**, 1025.
10 H. M. Rietveld, *J. Appl. Crystallogr*., 1969, **2**, 65.
11 A. Larson, R. B. von Dreele, *GSAS [General Structure Analysis System] Manual*; Los Alamos Scientific Laboratory Report No. LA-UR-86-748; Los Alamos Scientific Laboratory: Los Alamos, NM, 1986.
12 J. B. Hastings, W. Thomlinson and D. E. Cox, *J. Appl. Crystallogr.*, 1984, **17**, 85.
13 A. L. Spek, *J. Appl. Crystallogr*., 2003, **36**, 7.
14 A. Alberti, G. Cruciani and I. Dauru, *Eur. J. Mineral*., 1995, **7**, 501.
15 K. *Z.* Sahl, *Kristallogr*., 1980, **152**, 13.
16 J. F. Stebbins, P. Zhao, S. K. Lee and X. Cheng, *Am. Mineral.*, 1999, **84**, 1680.
17 X. Cheng, P. Zhao and J. F. Stebbins, *Am. Mineral.*, 2000, **85**, 1030.
18 S. B. Hong, S. H. Kim, Y. G. Kim, Y. C. Kim, P. A. Barrett and M. A. Camblor, *J. Mater. Chem*., 1999, **9**, 2287.
19 S. J. Warrender, P. A. Wright, W. Zhou, P. Lightfoot, M. A. Camblor, C.-H. Shin, D. J. Kim and S. B. Hong, *Chem. Mater*., 2005, **17**, 1272.
20 S. J. Warrender, P. A. Wright, W. Zhou, P. Lightfoot, M. A. Camblor, C.-H. Shin, D. J. Kim and S. B. Hong, *Stud. Surf. Sci. Catal*., 2005, **158**, 89.
21 B. Han, C.-H. Shin, S. J. Warrender, P. Lightfoot, P. A. Wright, M. A. Camblor and S. B. Hong, *Chem. Mater*., 2006, **18**, 3023.
22 K. G. Strohmaier and D. E. W. Vaughan, *J. Am. Chem. Soc*., 2003, **125**, 16035.
23 M. A. Camblor, S. B. Hong and M. E. Davis, *Chem. Commun.*, 1996, 425.
24 S. B. Hong, M. A. Camblor and M. E. Davis, *J. Am. Chem. Soc.*, 1997, **119**, 761.
25 Y. Lee, S. J. Kim and J. B. Parise, *Microporous Mesoporous Mater*., 2000, **34**, 255.
26 Y. Lee, S. J. Kim, I. Bull, A. J. Celestian, J. B. Parise, C.-C. Kao and T. Vogt, *J. Am. Chem. Soc.*, 2007, **129**, 13744.
27 Szostak, R. *Stud. Surf. Sci. Catal*., 2001, **137**, 89.V. Kahlenberg, J. B. Parise, Y. Lee and A. Tripathi, *Z. Kristallogr*.2002, **217**, 249. G. Lampert and R. Bohme, *Z. Krystallogr*., 1986, **176**, 29.
28 P. A. Sandomirskii, S. S. Mashalkin, I. V. Rozhdestvenshaya, L. N. Dem'yanets and T. G. Uvarova, *Sov. Phys. Crystallogr. (Engl. Transl.)*, 1986, **31**, 522.
29 W. A. Dollase and W. P. Freeborn, *Am. Mineral.*, 1977, **62**, 336.
30 M. Andreatschke, K. Range, H. Haase and U. *Z.* Klement, *Naturforsch. B*, 1992, **47**, 1249.
31 M. Lujon, F. Kubel and H. *Z.* Schmid, *Naturforsch. B*, 1994, **49**, 1256.
32 J. Barbier and M. E. Fleet, *J. Solid State Chem*., 1987, **71**, 361.

Supplementary Material (ESI) for Dalton Transactions

Supplementary Information

for

Synthesis and *in situ* transformation of PST-1: a potassium gallosilicate natrolite with a high Ga content

Jiho Shin,[a] Seok Han Kim,[a] Miguel A. Camblor,[b] Stewart J. Warrender,[c] Stuart R. Miller,[c] Wuzong Zhou,[c] Paul A. Wright[c] and Suk Bong Hong[*a]

[a] *School of Environmental Science and Engineering and Department of Chemical Engineering, POSTECH, Pohang 790-784, Korea. E-mail: sbhong@postech.ac.kr*
[b] *Instituto de Ciencia de Materiales de Madrid, Consejo Superior de Investigaciones Científicas (CSIC), C/Sor Juana Inés de la Cruz, 3, 28049 Madrid, Spain*
[c] *School of Chemistry, University of St. Andrews, Purdie Building, North Haugh, St. Andrews KY16 9ST, UK*

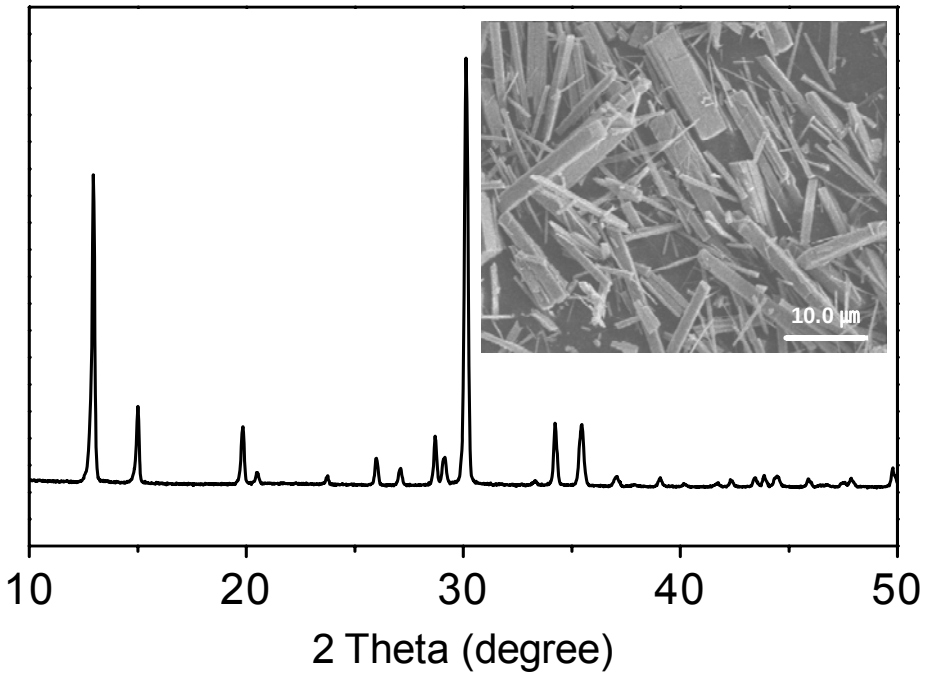

Fig. S1 Powder XRD pattern and SEM image of PST-1 obtained by heating a synthesis mixture with SiO_2/Ga_2O_3 = 5 and K_2O/SiO_2 = 0.8 under rotation (60 rpm) at 150 ºC for 2 days.

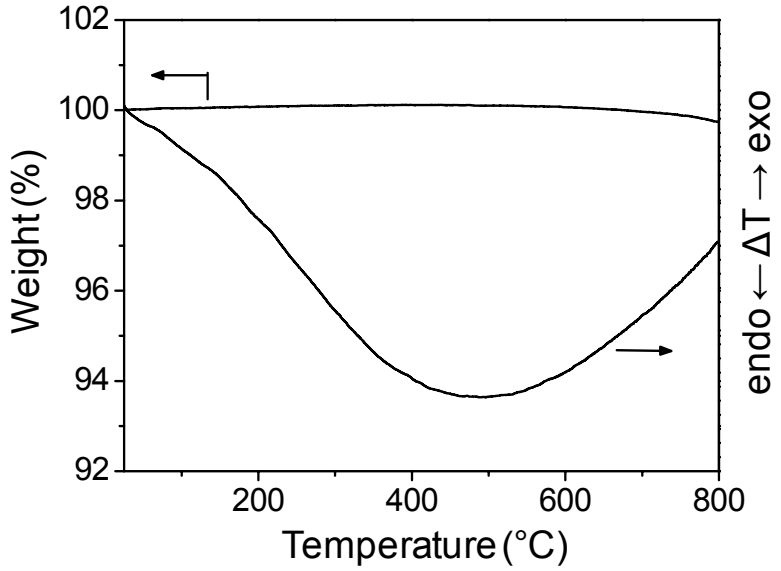

Fig. S2 TGA/DTA curves for TNU-6.

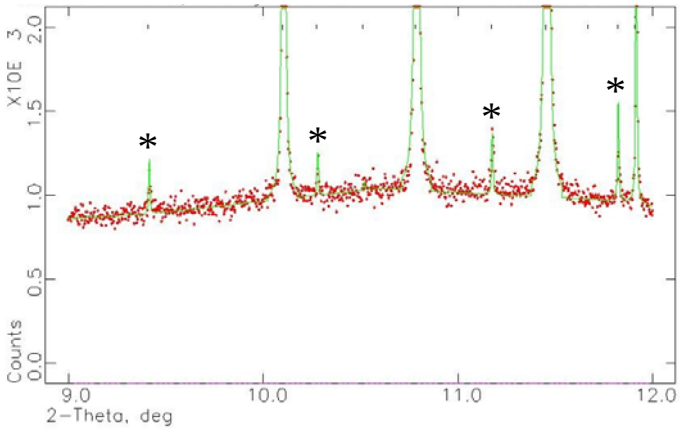

Fig. S3 Synchrotron powder diffraction data for TNU-6. The supercell reflections are marked by asterisks.

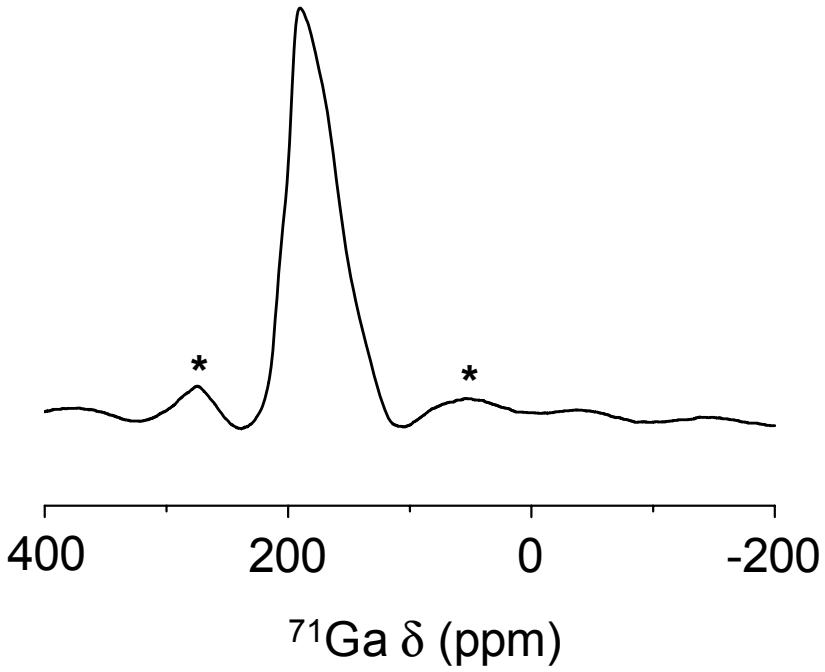

Fig. S4 ^{71}Ga MAS NMR spectrum of TNU-6. Spinning side bands are marked by asterisks.